

Ray Theory vs the Parabolic Equation in a Long-Range Ducted Environment

A. TOLSTOY, E. R. FRANCHI, AND K. R. NICOLAS

*Large Aperture Acoustics Branch
Acoustics Division*

August 22, 1983



NAVAL RESEARCH LABORATORY
Washington, D.C.

SECURITY CLASSIFICATION OF THIS PAGE (When Data Entered)

REPORT DOCUMENTATION PAGE		READ INSTRUCTIONS BEFORE COMPLETING FORM						
1. REPORT NUMBER NRL Report 8730	2. GOVT ACCESSION NO.	3. RECIPIENT'S CATALOG NUMBER						
4. TITLE (and Subtitle) RAY THEORY VS THE PARABOLIC EQUATION IN A LONG-RANGE DUCTED ENVIRONMENT		5. TYPE OF REPORT & PERIOD COVERED Interim report on a continuing NRL problem.						
		6. PERFORMING ORG. REPORT NUMBER						
7. AUTHOR(s) Alexandra Tolstoy, Edward R. Franchi, and Kenneth R. Nicolas		8. CONTRACT OR GRANT NUMBER(s)						
9. PERFORMING ORGANIZATION NAME AND ADDRESS Naval Research Laboratory Washington, DC 20375		10. PROGRAM ELEMENT, PROJECT, TASK AREA & WORK UNIT NUMBERS 62759N XF59-552-500						
11. CONTROLLING OFFICE NAME AND ADDRESS Naval Electronic Systems Command Washington, DC 20360		12. REPORT DATE August 22, 1983						
		13. NUMBER OF PAGES 27						
14. MONITORING AGENCY NAME & ADDRESS (if different from Controlling Office)		15. SECURITY CLASS. (of this report) UNCLASSIFIED						
		15a. DECLASSIFICATION/DOWNGRADING SCHEDULE						
16. DISTRIBUTION STATEMENT (of this Report) Approved for public release; distribution unlimited.								
17. DISTRIBUTION STATEMENT (of the abstract entered in Block 20, if different from Report)								
18. SUPPLEMENTARY NOTES								
19. KEY WORDS (Continue on reverse side if necessary and identify by block number)								
<table> <tbody> <tr> <td>Acoustic propagation</td> <td>Surface duct</td> </tr> <tr> <td>Ray theory</td> <td>Model comparisons</td> </tr> <tr> <td>Parabolic equation</td> <td>Analytic profiles</td> </tr> </tbody> </table>			Acoustic propagation	Surface duct	Ray theory	Model comparisons	Parabolic equation	Analytic profiles
Acoustic propagation	Surface duct							
Ray theory	Model comparisons							
Parabolic equation	Analytic profiles							
20. ABSTRACT (Continue on reverse side if necessary and identify by block number)								
<p>An important type of underwater acoustic environment involves a deep-water SOFAR channel with a superimposed (winter) surface duct capable of trapping acoustic energy. In this report we examine the effects predicted by a computer model of three ducted sound-speed profiles and two analytic profiles on acoustic propagation at 300 Hz. The purpose of this study was to better understand the capabilities and limitations (both theoretical and numerical) of a ray-theoretic model for predicting mid- and long-range signal transmission loss (TL) in the</p> <p style="text-align: right;">(Continued)</p>								

DD FORM 1473
1 JAN 73EDITION OF 1 NOV 65 IS OBSOLETE
S/N 0102-014-6601

SECURITY CLASSIFICATION OF THIS PAGE (When Data Entered)

20. ABSTRACT (Continued)

winter North Atlantic. Several source and receiver configurations (combinations with one or both in and out of the duct) have been studied. To test validity, the ray-theoretic calculations are compared to previously accepted results predicted by a propagation model based upon the parabolic equation. Both model predictions agree qualitatively (TL measurements and acoustic field patterns are comparable), while any quantitative discrepancies are explained by the theoretical or numerical limitations of the different approaches. We conclude that when both the source and receiver are at least several wavelengths from the sea surface, ray theory can be quite accurate in its predictions for these ducted environments.

CONTENTS

INTRODUCTION	1
TEST DATA	2
RESULTS	2
CONCLUSIONS	10
REFERENCES	12
APPENDIX A – PE Background	13
APPENDIX B – Ray Theory Background	16
APPENDIX C – Analytic Profile Results	21

RAY THEORY VS THE PARABOLIC EQUATION IN A LONG-RANGE DUCTED ENVIRONMENT

INTRODUCTION

An important type of underwater acoustic environment involves a deep water SOFAR channel with a superimposed surface duct capable of trapping acoustic energy. While considered to be most representative of winter conditions (the profiles contain no surface heating effects), this environment prevails over northern latitude areas throughout the year and is adequate for the intended parameter study. In this report, we examine the effects on acoustic propagation predicted by a computer model of three ducted sound-speed profiles for a nominal frequency of 300 Hz. The purpose of this study was to better understand the capabilities and limitations (both theoretical and numerical) of a ray-theoretic model for predicting mid- and long-range signal transmission loss (TL) in strong surface ducts, for example as in the winter North Atlantic. Several source and receiver configurations (combinations with one or both in and out of the duct) have been studied. To test validity, the ray-theoretic calculations are compared to previously accepted results predicted by a propagation model based upon the parabolic equation (PE). Both model predictions agree to first order (TL measurements and acoustic field patterns are comparable), while any second-order discrepancies are explained by the theoretical or numerical limitations of the different approaches. We conclude that when both the source and receiver are at least several wavelengths from the sea surface,* ray theory can be accurate in its predictions for these ducted environments.

Study Motivation

This study is concerned with assessing the capabilities and limitations of ray-theoretic models when used to predict mid- and long-range signal behavior in deep-water environments with superimposed surface ducts. The ray-theoretic model is one which has been incorporated as a submodel into the NRL reverberation model [2]. The PE model used for this study is one that has also been developed at NRL [3].

In general, the PE method (Appendix A) has achieved widespread acceptance in the acoustics community because of its versatility over a large frequency domain and under many environmental conditions. However, such an approach is not always appropriate or practical, particularly when the time-dependence of a pulse signal and when backscattered energy must be considered as in reverberation studies. An alternate method often used is the ray-theoretic approach (Appendix B). Ray theory has a number of advantages over the PE method for computing reverberation in long-range active sonar applications. These advantages are:

- It easily computes time of arrival for pulsed signals.
- Models for backscattering and forward scattering of energy can be easily incorporated.
- There is no limitation on the propagation angles which can be considered.

Manuscript approved March 31, 1982.

*When source and receiver are at the surface, an unmanageable piling up of caustics as range increases results in the complete breakdown of ray theory [1]. The results show no such difficulties for a source at 91 m receiver of 20 m to ranges of 150 nmi.

The propagation model used in this study is a corrected ray-theoretic model which overcomes the normal difficulties with caustics and discontinuities in derivatives of the sound-speed profile. The model incorporates a correction for smooth caustics [4] based upon a uniform asymptotic expansion for the inverse Hankel transform of the WKB solution of the Hankel transformed wave equation. The solution can be extended into the caustic shadow zone to predict appropriate nonzero intensities. Moreover, the sound-speed profile data points are fit by a cubic spline interpolating polynomial to ensure good behavior for the first and second depth derivatives.

The ray-theoretic model can be expected to have limitations at low frequencies, under conditions of strong sound-speed gradients, and when diffraction and mode coupling effects are dominant. However, the extent to which these disadvantages limit the applicability of a medium- to long-range reverberation model incorporating a corrected ray-theoretic propagation submodel needs to be addressed. This study was motivated by the belief that a ray-based reverberation model could provide reasonable calculation results for long-range active sonars under a variety of important environmental conditions, including strong winter surface ducts. This study is aimed at assessing such a capability by comparing the propagation results from the two models for environmental conditions in which the PE method had been used in a previous study and for which those results have received wide acceptance. Our study uses the same sound-speed environments as the previous PE studies, but only some of the source-receiver placements. Thus, this study is not an exhaustive investigation, but one in which a number of conditions of general interest are explored. The objective is to see how well a ray-theoretic propagation model will work in situations where it would be practical to use such a model as part of a reverberation prediction capability. Frequently such ray-based approaches to reverberation estimation are dismissed without quantitative justification even though, they can achieve good accuracy and save computer time.

TEST DATA

Three ducted environments selected from measured data have been considered for this study. Their surface ducts range from 200 m to 800 m in depth while the total water depth is a constant 3000 m. Although the ray program can handle variations of bottom topography and sound speed with range, we elected to examine only flat bottom and range-independent environments. In this manner we could most confidently deduce the causes of any propagation discrepancies. See Fig. 1 and Table 1 for the profiles selected for this study and the comparison of properties of the sound-speed profiles. The source depths selected were 91 m and 305 m while receiver depths were at 20, 50, 90, and 306 m; we also presume a point source with a 300-Hz constant frequency. For waveguide boundaries we assume a totally absorbing, liquid bottom and a flat, totally reflecting (with phase change of π) sea-surface. Note that the shallowest duct considered here is still some 40 wavelengths deep, and the maximum gradient dc/dz computed for all profiles was about 0.027 s^{-1} . Thus, $0.027/300 \ll 4\pi$ implies that ray-theory applicability is not contraindicated.

RESULTS

Figures 2a to 7a represent PE signal intensity plots for profiles 1, 2, and 3 as indicated with source depths located at 91 m and 305 m. Figures 2b to 7b represent the corresponding ray traces. In the PE figures, the pronounced and genuine (measurable) interference patterns (the shading with dark regions indicating high intensity). These patterns are produced by the coherent addition of the PE modes/rays. The ray figures display more diagrammatic patterns or ray tracks since the intensity calculations are performed at a later stage in the program's computations. However, a number of conclusions may still be drawn by comparison between these ray and PE plots. First, for profiles 1 and 2 (Figs. 2 to 5) both types of plots indicate significant levels of energy trapped in the surface duct. Next, they both indicate the presence of deep cycling energy which has escaped the surface duct and which displays decreasing focusing (more smearing out) with increasing range from the sources. Examining the behavior elicited by profile 3 (Figs. 6 and 7) we note that for this shallower surface duct (200 m deep), the source at 305 m is located below the duct. As a result, little signal energy becomes trapped near the surface. Finally,

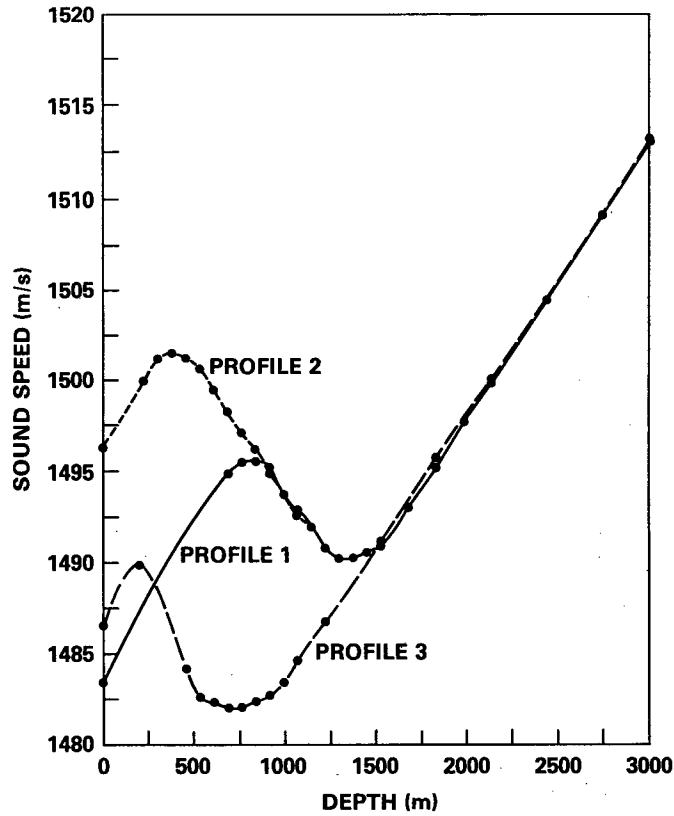


Fig. 1 — Three ducted sound-speed profiles. Data points are indicated by points with spline interpolation used between them.

Table 1 — Comparison of Properties of Sound-Speed Profiles

Property	P1	P2	P3
Surface duct depth (m)	800	381	200
SOFAR axis depth (m)	1334	1334	724
Ocean depth (m)	3000	3000	3000
Sound speed at the ocean surface (m/s)	1483	1496	1487
Sound speed at surface duct maximum (m/s)	1495	1501	1490
Sound speed at SOFAR axis (m/s)	1490	1490	1482
Sound speed at ocean bottom (m/s)	1512	1512	1512

we see that all the PE figures agree extremely well with the ray figures in the fine detail of the signal structure, and indeed, if these plots are overlaid, it becomes apparent that the patterns are in excellent alignment with each other. To understand conditions under which noticeable shifts in such patterns might occur (between the ray and PE approaches) we also considered the effects of two strongly refracting analytic sound-speed profiles. Appendix C contains these results.

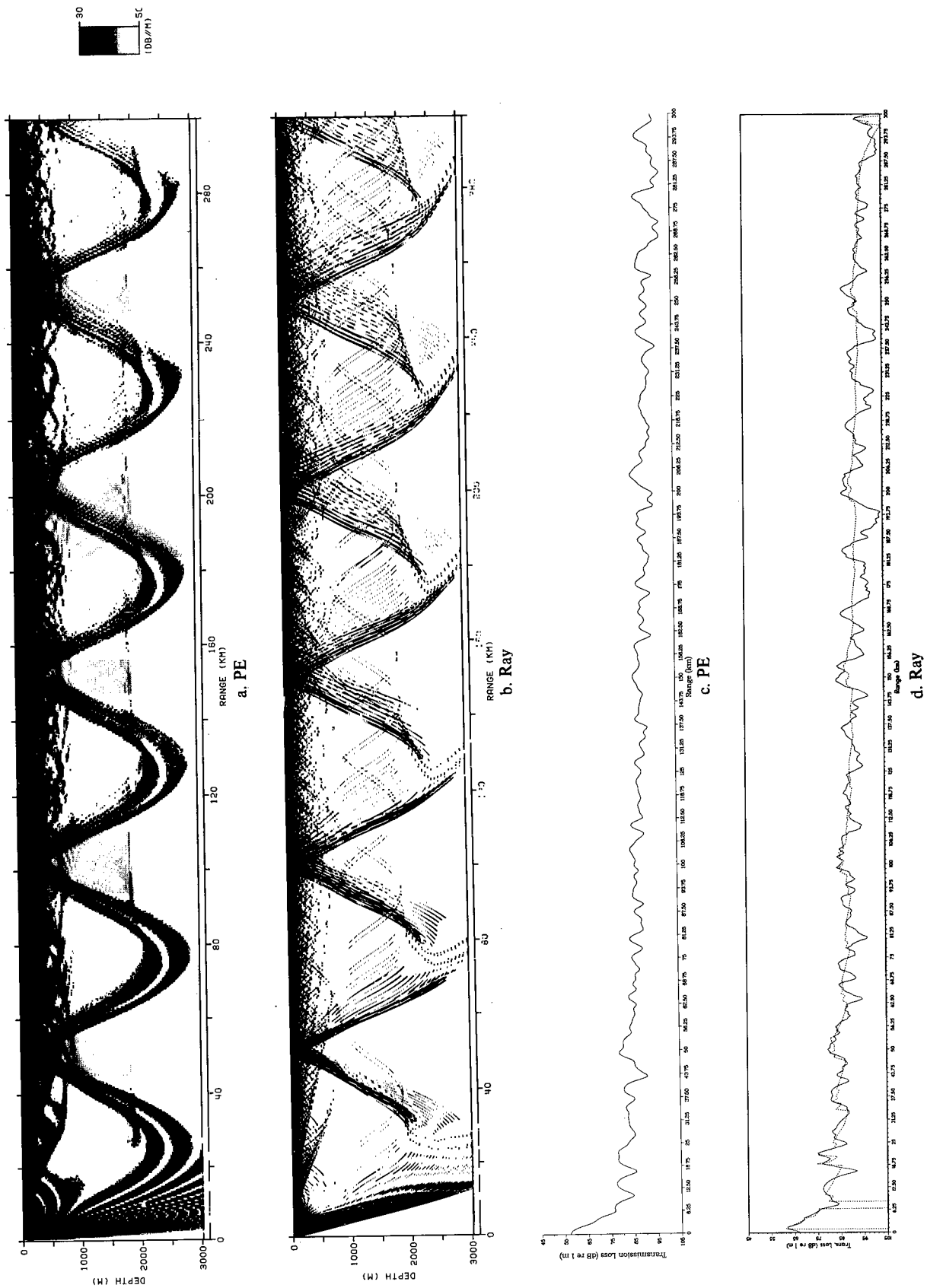


Fig. 2 — Ray tracks, PE intensity plots and transmission loss plots as a function of range for sound speed profile 1 with SD = 91 m, RD = 305 m, 300 Hz

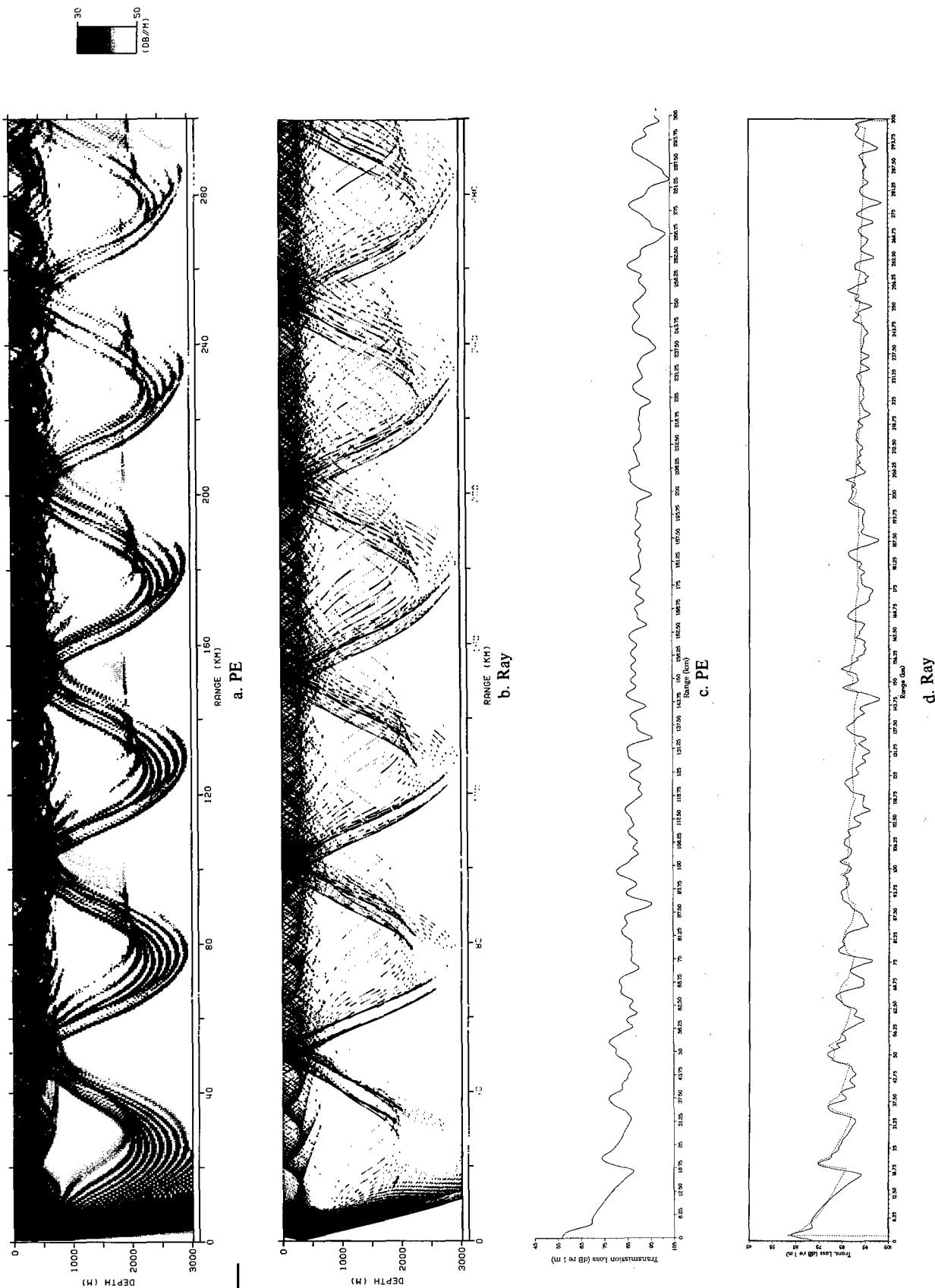


Fig. 3 - Ray tracks, PE intensity plots and transmission loss plots as a function of range for sound speed profile 1 with SD = 305 m, RD = 20 m, 300 Hz

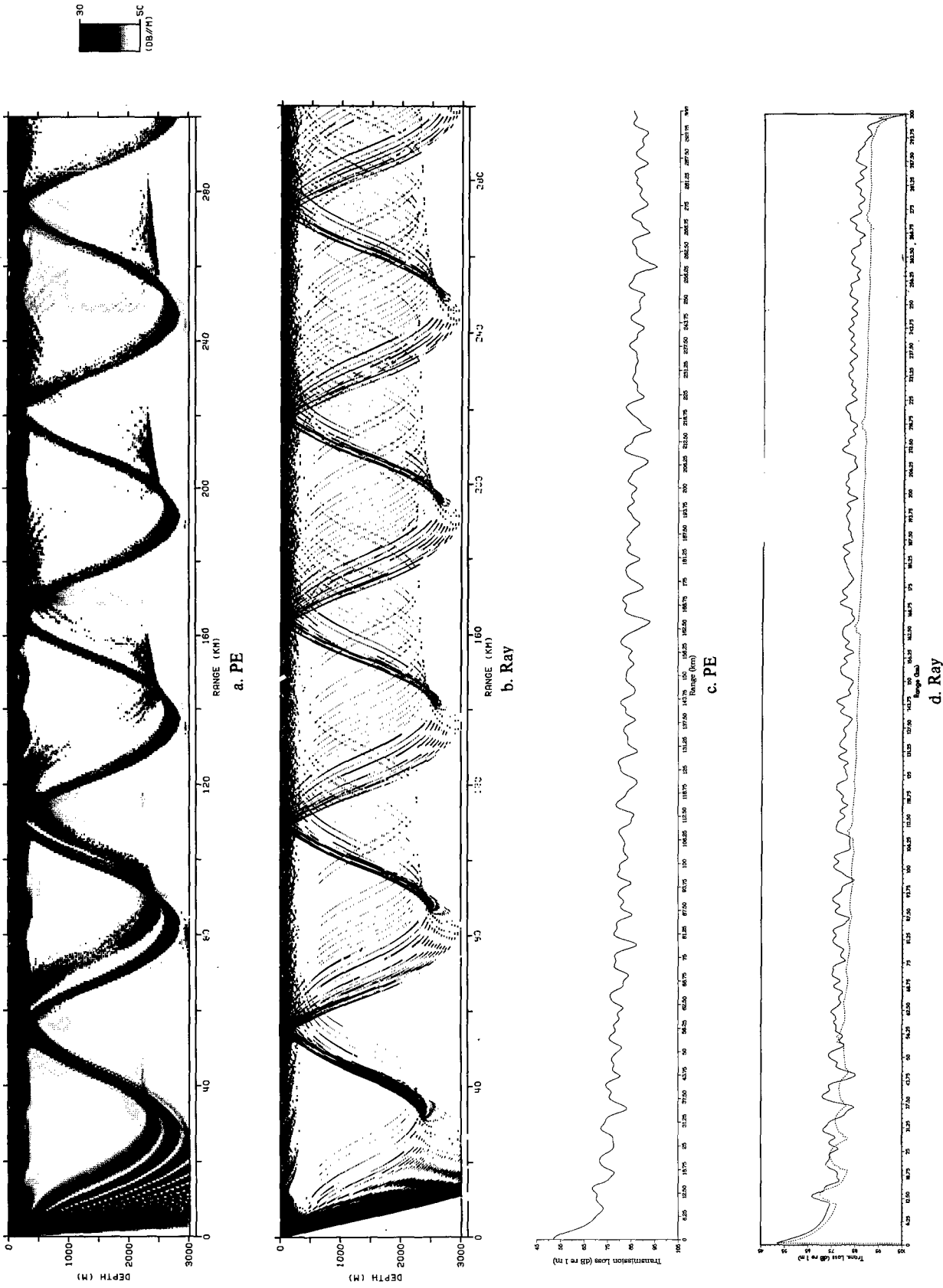


Fig. 4 — Ray tracks, PE intensity plots and transmission loss plots as a function of range for sound speed profile 2 with SD = 91 m, RD = 20 m, 300 Hz

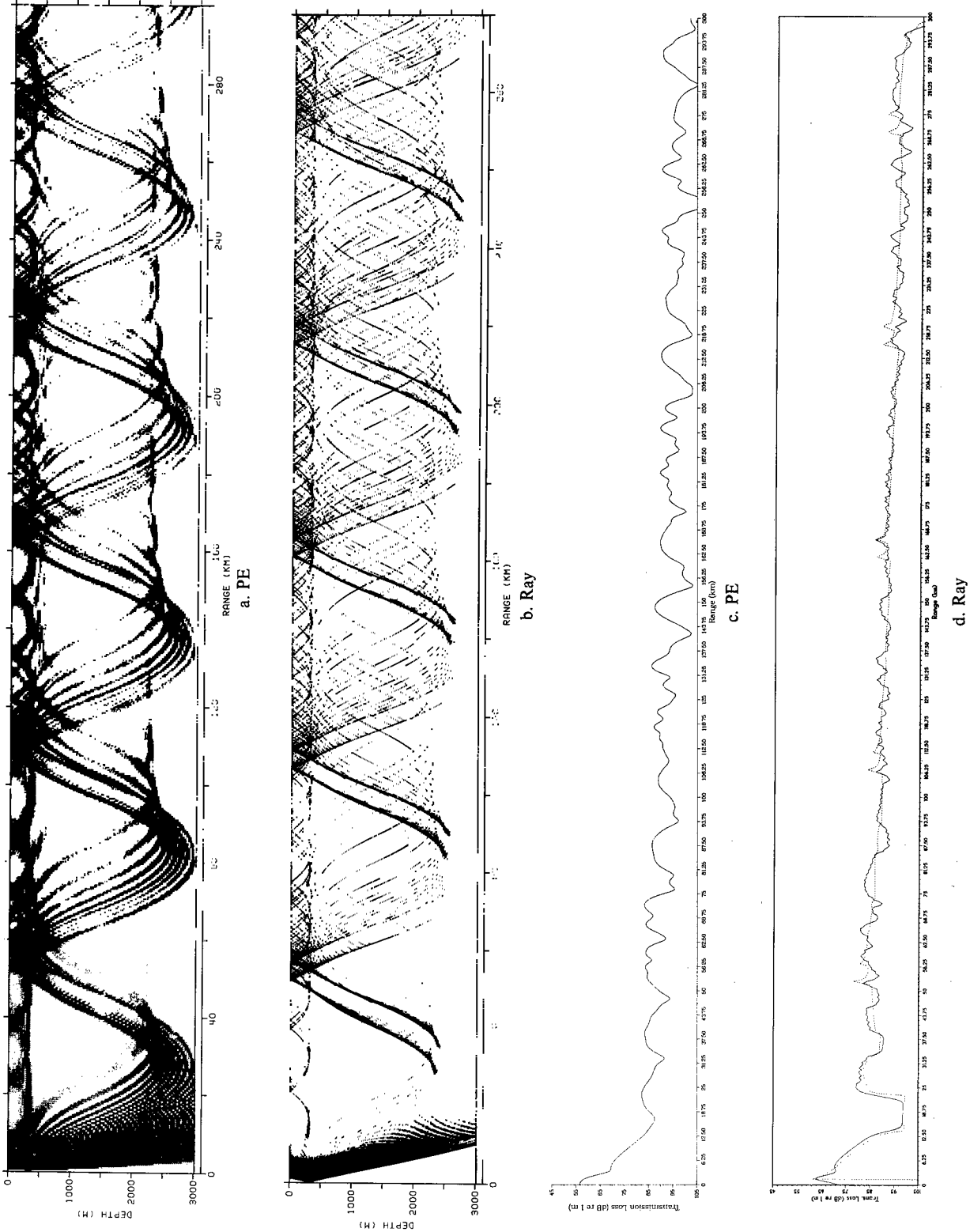


Fig. 5 — Ray tracks, PE intensity plots and transmission loss plots as a function of range for sound speed profile 2 with SD = 305 m, RD = 20 m, 300 Hz

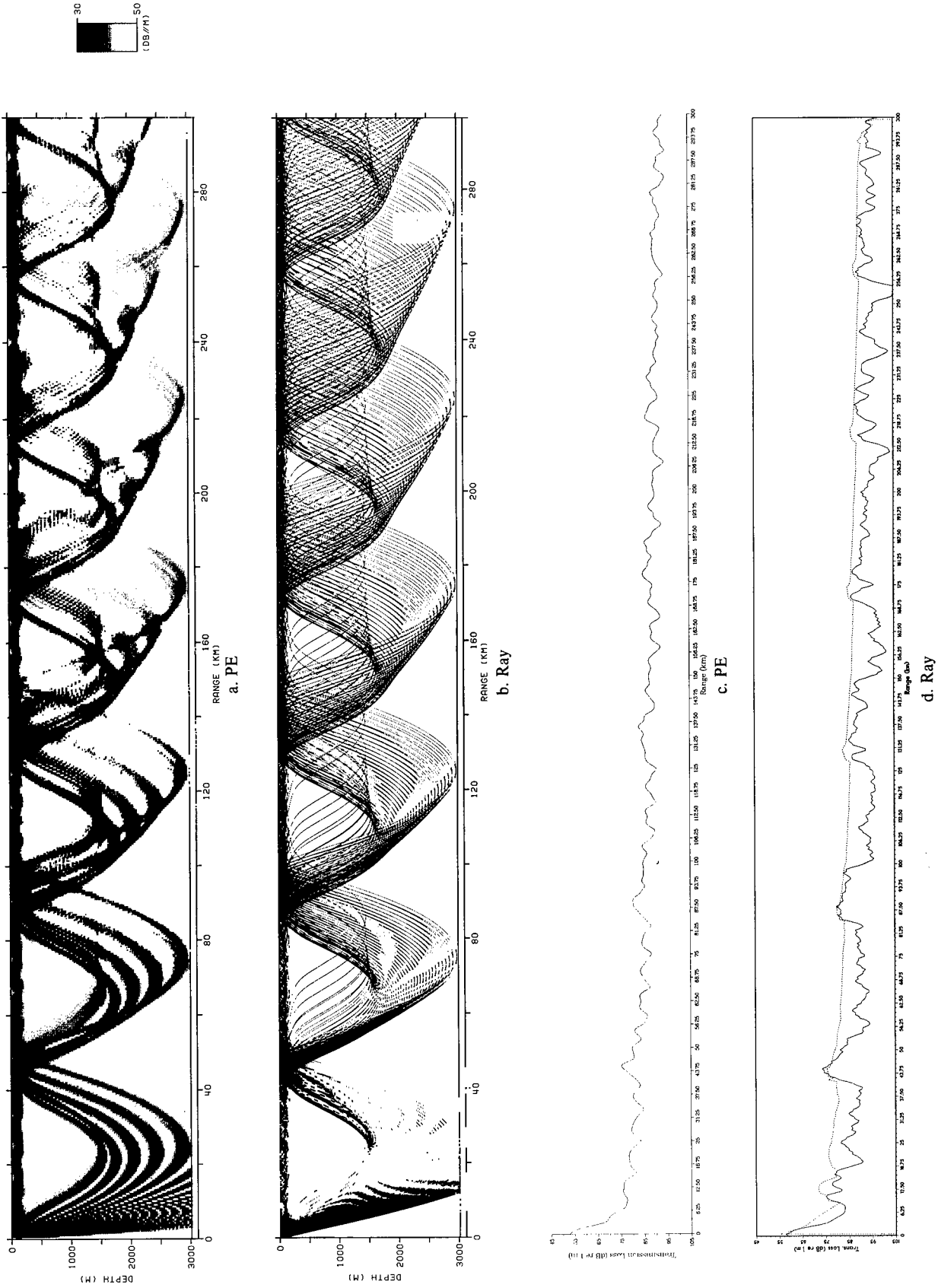


Fig. 6 — Ray tracks, PE intensity plots and transmission loss plots as a function of range for sound speed profile 3 with SD = 91 m, RD = 50 m, 300 Hz

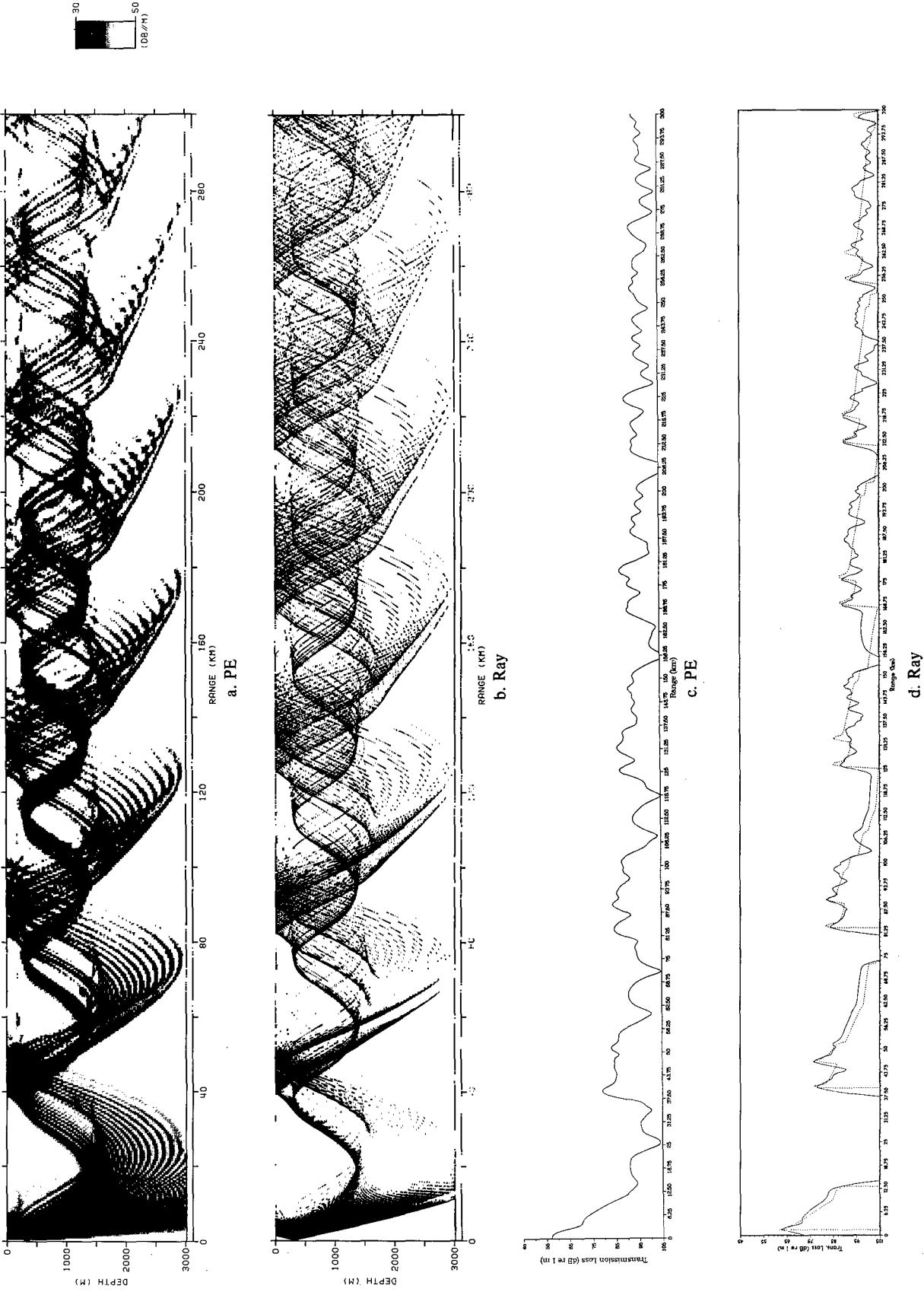


Fig. 7 — Ray tracks, PE intensity plots and transmission loss plots as a function of range for sound speed profile 3 with SD = 305 m, RD = 20 m, 300 Hz

Next, we examined predicted levels of signal transmission loss vs range (at a specified receiver depth). These levels are plotted in both raw and range averaged (Gaussian weights over $6\sigma = 5$ km) forms. In Figs. 2c-7c and 8a the ray model plots now represent both an incoherent* (dashed line) and a coherent sum of ray intensities. We can expect some disagreement between the two models at ranges near the source (within 20 km) because the PE approximation is expected to acquire validity only at longer ranges (we recall the far-field and paraxial assumptions). In addition, for the ray model the density of rays has been limited deliberately at the higher (more vertical) launch angles which can sometimes result in unrealistic zero intensities (large TL) in the short range unaveraged/raw data (see Fig. 8 in the ranges 5 to 10 km). This sparsity should not be regarded as more than a temporary and inconsequential aberration. That is, the high-angle rays which would be included for a more accurate near-field effect eventually interact often enough with the bottom to become absorbed and thereby not affect results at the longer ranges which are the focus of this study. For profile 3, source depth 305 m, receiver depth 20 m we again note zero intensity levels in the ray model predictions (Fig. 7d). However, we note here that the gap is rather extended in range (≤ 20 km) and reappears several times (ranges 13 to 38, 60 to 80, 113 to 125 km) before the deep cycling energy smears out sufficiently near the surface to introduce consistently nonzero intensity levels. These gaps (for a receiver in the duct, source below the duct or vice-versa) are due primarily to the failure of the ray theoretic approach to consider diffracted energy. Note, however, that these gaps would have been partially filled if bottom-reflected energy had been considered (a more realistic situation).

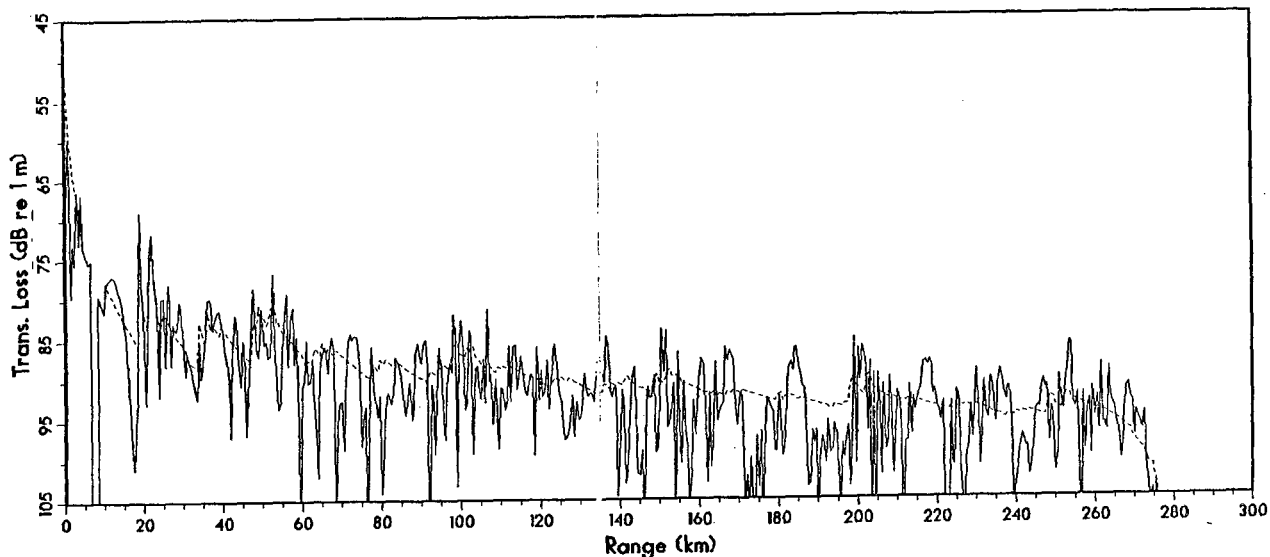
We conclude that the levels of transmission loss vs range predicted by the two models are in good agreement (see Figs. 2c, 2d, 7c, 7d, 8). Both models involve different theoretical as well as numerical approximation to the exact solution. Consequently, we should not expect the detailed interference patterns; that is, the location of signal maxima and minima, as predicted by each model to agree, particularly as range increases. In the raw data, where the oscillations are quite frequent, a statistical comparison would be required to show how well the two models agree or disagree with regard to fine structure. It is to be expected that the PE and ray-theoretic approaches should not, in fact, yield the exactly identical responses to any given environment. Indications of when and how the two solutions can differ may be found in Appendix C where two analytical profiles are considered.

CONCLUSIONS

For the test cases examined, the ray model and the PE model agree extremely well. In particular, the ray tracks and PE intensity plots show excellent and detailed correlation in the ducted- and deep-cycling energy. The range-averaged TL levels also agree except under some near-field conditions where either the lack of a sufficient number of high-angle rays or the lack of consideration of diffraction effects in the ray model has occasionally led to levels which are unrealistically low. Thus, the few occasions on which the two approaches differed are well understood. Since the focus of this study is on long-range prediction, these areas of disagreement are not considered serious. As a result, we believe that long-range predictions as made by the extended ray model used in this report should be as accurate as PE predictions in ducted environments with $\lambda < h/10$ and for sources and receivers away from the sea-surface.

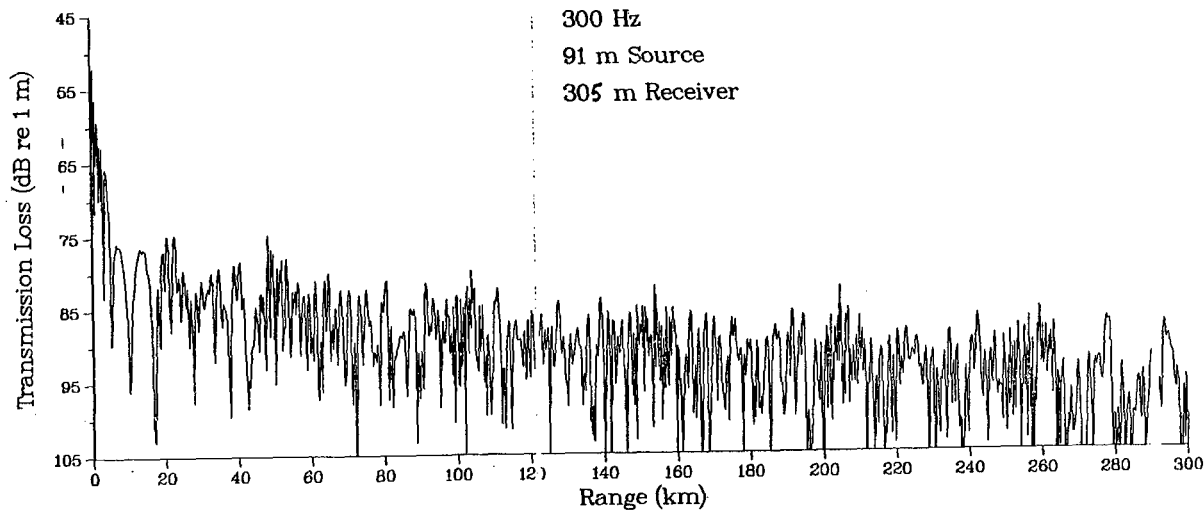
*This is essentially a weighted (Gaussian in range and centered about the receiver location) sum of ray intensities at each depth [2,5].

profile 1 300 Hz sd=91m rd=305m



(a)

PROFILE 1



(b)

Fig. 8 — Unaveraged transmission loss as a function of range (a: ray theoretic; b: PE theoretic) for sound speed profile 1 with SD = 91 m, RD = 305 m, freq = 300 Hz.

REFERENCES

1. L.B. Felsen and T. Ishihara, "Hybrid ray-mode formulation of ducted propagation," *JASA* **65**(3) 595-607 (1979).
2. E.R. Franchi, J.M. Griffin, and B.J. King, "NRL Reverberation Model: A Computer Program for the Prediction and Analysis of Medium to Long Range Boundary Reverberation," NRL Report in press.
3. J.S. Perkins and R.N. Baer, "A Corrected Parabolic-Equation Program Package for Acoustic Propagation," NRL Memorandum Report 3688, 1978, ADA-050-564.
4. D.A. Sachs and A. Silbiger, "Focusing and Refraction of Harmonic Sound and Transient Pulses in Stratified Media," *JASA* **49**(3), 824-840 (1971).
5. J.J. Cornyn, "GRASS: A Digital-Computer Ray-Tracing and Transmission-Loss-Prediction System, Volume I – Overall Description," NRL Report 7621, 1973, AD-781-230.

Appendix A PE BACKGROUND

By linearizing both the Navier-Stokes' equation for a nonviscous fluid (Newton's equation of motion), and the equation of continuity (conservation of mass), one finds that to a good first approximation, propagation of small amplitude sound waves in an ocean environment can be described by the linear, hyperbolic, second-order, time-dependent, scalar wave equation [A1,A2]:

$$\nabla^2 \psi - \frac{1}{c^2(\vec{x})} \frac{\partial^2 \psi}{\partial t^2} = -f(\vec{x}, t), \quad (\text{A1})$$

where ψ is the acoustic pressure perturbation,
 \vec{x} is the position vector in a 3-dimensional coordinate system,
 $c(\vec{x})$ is the sound speed profile (assumed time-independent), and
 $f(\vec{x}, t)$ is the source function.

By using appropriate boundary and initial conditions (BCs and ICs) one is guaranteed the existence of a unique solution in some appropriate solution space. However, as $c(\vec{x})$ or the BCs become complicated, it becomes impossible to compute an exact analytic solution. Hence, schemes to approximate this solution have been developed, one of which is the parabolic approximation.

Let us now consider a two-dimensional environment with cylindrical coordinates (r, z) where r is range, z is depth ($z = 0$ at sea surface, $z > 0$ below surface). Then for harmonic time dependence the wave equation becomes the Helmholtz (reduced) wave equation:

$$\nabla^2 \psi(r, z) + k_0^2 n^2(r, z) \psi(r, z) = -f(r, z) \quad (\text{A2})$$

where k_0 is the reference wave number,
 $n(r, z)$ is the index of refraction,
 $= \omega / (k_0 c(\vec{x}))$, and
 ω is the source angular frequency.

We can write the Green's function solution ($f = \delta(r) \delta(z - z_0)$) as

$$\psi(r, z) = \frac{e^{ik_0 r}}{\sqrt{r}} \phi(r, z), \quad (\text{A3})$$

where ϕ satisfies (away from the source):

$$\frac{\partial^2 \phi}{\partial r^2} + 2ik_0 \frac{\partial \phi}{\partial r} + \frac{\partial^2 \phi}{\partial z^2} + k_0^2 \left[n^2(r, z) - 1 + \frac{1}{4k_0^2 r^2} \right] \phi = 0. \quad (\text{A4})$$

If we now assume that

$$\left| \frac{\partial^2 \phi}{\partial r^2} \right| \ll \left| 2k_0 \frac{\partial \phi}{\partial r} \right| \quad (\text{A5})$$

and that

$$\frac{\phi}{r^2} \approx 0 \quad (\text{far field}), \quad (\text{A6})$$

then

$$2ik_0 \frac{\partial \phi}{\partial r} + \frac{\partial^2 \phi}{\partial z^2} + k_0^2 (n^2(r, z) - 1) \phi \approx 0. \quad (\text{A7})$$

Equation (A5) is usually referred to as the paraxial approximation which implies that if the acoustic field were represented by rays then these would be included only at small angles with respect to the horizontal [A3-A5].

A solution to Eq. (A7) may be found simply by Fourier transforming the equation (on z) and then assuming that

$$n(r,z) \approx \text{constant}, \quad (\text{A8})$$

$$\phi, \frac{\partial \phi}{\partial z} \rightarrow 0 \text{ as } z \rightarrow \infty, \quad (\text{A9})$$

then integrating by parts to obtain

$$\frac{\partial \Phi}{\partial r} + \frac{k_0^2 (n^2 - 1) - s^2}{2ik_0} \Phi = 0, \quad (\text{A10})$$

where

$$\Phi(r,s) \stackrel{\text{def}}{=} \frac{1}{2\pi} \int_{-\infty}^{\infty} \phi(r,z) e^{isz} dz. \quad (\text{A11})$$

Then,

$$\frac{\frac{\partial \Phi}{\partial r}}{\Phi} = \frac{s^2 - k_0^2 (n^2 - 1)}{2ik_0}. \quad (\text{A12})$$

So, integrating from r to $r + \Delta r$ we have

$$\ln \left\{ \frac{\Phi(r + \Delta r, s)}{\Phi(r, s)} \right\} = \Delta r \left\{ \frac{s^2 - k_0^2 (n^2 - 1)}{2ik_0} \right\} \quad (\text{A13})$$

implying

$$\Phi(r + \Delta r, s) = \Phi(r, s) \exp \left[\frac{i\Delta r}{2} \left\{ k_0 (n^2 - 1) - \frac{s^2}{k_0} \right\} \right]. \quad (\text{A14})$$

This equation can be inverse transformed to obtain

$$\phi(r + \Delta r, z) = e^{ik_0(n^2 - 1)\Delta r} \frac{\Delta r}{2} F^{-1} \left\{ e^{-is^2 \frac{\Delta r}{2k_0}} \Phi(r, s) \right\} \quad (\text{A15})$$

where

$$F^{-1}\{f\} \stackrel{\text{def}}{=} \int_{-\infty}^{\infty} f(s) e^{-isz} ds. \quad (\text{A16})$$

Thus, the field at any range $(r + \Delta r)$ depth z is obtained by stepping the solution by a range increment Δr from the earlier value at range r , depth z .

Theoretically and numerically this solution is stable and highly accurate even when $n(r,z)$ is not constant provided Δr is sufficiently small [A4]. Within the conditions of its application, this treatment includes all effects normally associated with diffraction and mode coupling in a range and depth dependent environment, but does not allow for the backscattering of acoustic energy or for the propagation of high angle rays. The sea-surface ($z = 0$) boundary condition of perfect reflection plus a phase change of π ($\phi = 0$ at $z = 0$) is replaced by an image source at $z = -z_0$. Also, for $|z| >$ bottom depth, n^2 is given an exponentially increasing imaginary part resulting in a solution which damps to zero as $|z| \rightarrow \infty$. An initial field ($r = 0$) must be computed before the marching algorithm (split-step) can begin operating on Eq. (A15), and this field has been calculated here as a very narrow Gaussian field for the assumed point source.

The PE model used [A5] has a number of attractive features.

- All frequencies can be accurately modeled by suitably choosing Δr .
- A range variable (as well as depth variable) environment can be considered.
- Diffraction and mode coupling effects are implicitly included.
- A choice of initial field is allowed, e.g., Gaussian, normal mode, user specified.
- Solution is highly stable.
- Sound speed profiles need only simple linear interpolation in depth between data points.

However, a PE approach also has its limitations.

- Time of arrival for pulsed signals (finite duration) cannot be computed.
- Backscattered energy is not allowed.
- The paraxial, that is small angle, approximation must be assumed (an acceptable assumption for most long range studies).
- Program requires large amounts of file storage for long range/high frequency calculations.

REFERENCES

- A1. P.M. Morse and K.U. Ingard, *Theoretical Acoustics*, McGraw-Hill Book Co., 1968.
- A2. K.M. Guthrie, "The Propagation of Sofar Signals," Phd thesis, University of Auckland, New Zealand, 1974.
- A3. Fock, V.A., *Electromagnetic Diffraction and Propagation Problems*, Pergamon Press, 1965.
- A4. F. Jensen and H. Krol, "The Use of the Parabolic Equation Method in Sound Propagation Modeling," SACLANTCEN Memo SM-72, La Spezia, Italy, 1975, ADA-016-847.
- A5. J.S. Perkins and R.N. Baer, "A Corrected Parabolic-Equation Program Package for Acoustic Propagation," NRL Memorandum Report 3688, 1978, ADA-050-564.

Appendix B RAY THEORY BACKGROUND

The geometrical approximation can be derived in a number of ways. One approach (we shall henceforth assume a harmonic time dependence) is to assume [B1] that the solution must be of a certain form, that is,

$$\psi(\vec{x}) = A(\vec{x}) e^{i(k_0 S(\vec{x}) - \omega t)} \quad (\text{B1})$$

where ω is the source angular frequency,
 k_0 is the reference wave number,
 $A(\vec{x})$ is the amplitude at \vec{x} , and
 $S(\vec{x})$ is the phase at \vec{x} .

Substituting this expression into the homogeneous wave equation $f(\vec{x}, t) = 0$ in Eq. (B1) and collecting real and imaginary terms leads to

$$\nabla^2 A - k_0^2 (S_x^2 + S_y^2 + S_z^2) A + \frac{\omega^2}{c^2(\vec{x})} A = 0, \text{ and} \quad (\text{B2})$$

$$2\nabla A \cdot \nabla S + A \nabla^2 S = 0 \text{ (transport equation)}. \quad (\text{B3})$$

If, we now assume that

$$\frac{\nabla^2 A}{A} \ll \frac{\omega^2}{c^2(\vec{x})} = k_0^2 n^2(\vec{x}), \quad (\text{B4})$$

where the index of refraction $n(\vec{x})$ is

$$n(\vec{x}) = \frac{\omega}{k_0 c(\vec{x})},$$

then Eq. (B2) becomes the standard eikonal equation (independent of source frequency):

$$|\nabla S|^2 = n^2. \quad (\text{B5})$$

We note that inequality Eq. (B4) may *not* hold.

- At too low frequencies (ω small), or
- for $\nabla^2 A$ large.

The computation of signal amplitude A (and subsequently, of $\nabla^2 A$) in ray theory proceeds either by solving Eq. (B3) when possible or by invoking the principle of conservation of energy flux for a ray bundle. If we assume constant density this leads to [B1]

$$A(\vec{x}_2) = \left\{ k_0 \frac{c(\vec{x}_2)}{c(\vec{x}_1)} \frac{d\sigma_1}{d\sigma_2} \right\}^{1/2} A(\vec{x}_1), \quad (\text{B6})$$

where $A(\vec{x}_i)$ is the field amplitude at \vec{x}_i , $i = 1, 2$
 $d\sigma_1$ is the ray bundle cross section at \vec{x}_i , $i = 1, 2$ (Fig. B1).

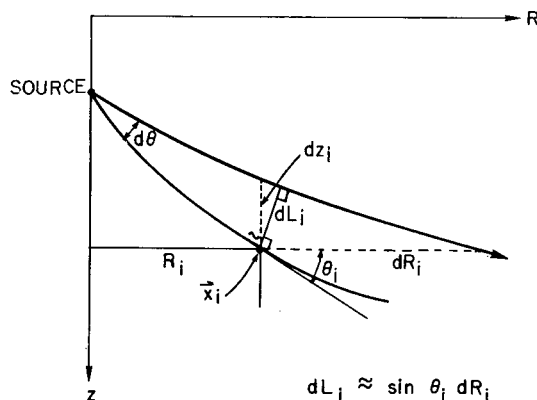


Fig. B.1 — Calculation of length dL_i of ray bundle cross section at \vec{x}_i

Clearly, Eq. (B6) predicts $A(\vec{x}_2) \rightarrow \infty$ (for $A(\vec{x}_1) < \infty$, $d\sigma_1 < \infty$) when $d\sigma_2 \rightarrow 0$. That is, ray theory does *not* hold:

near caustics and focal points.

On the basis of geometric arguments (Fig. B1) we have for a point source that

$$d\sigma_i \approx 2\pi R_i \sin\theta_i dR_i, \tag{B7}$$

where R_i is the horizontal distance from source to \vec{x}_i , and θ_i is the ray angle (w.r.t. horizontal) at \vec{x}_i .

Now, when $\theta = 0$, that is at the ray turning point, $\sin\theta \rightarrow 0$ and $dR \rightarrow \infty$. In this instance, however, the product has a well-defined limit, that is, $\sin\theta dR = \cos\theta dz = dz$ when $\theta \rightarrow 0$. Thus, for a *point source* ray theory gives accurate amplitude estimates at turning points. This is not true for a "plane-wave" (WKB) solution [B1] where the turning points lie on a caustic.

To obtain an alternate expression for $A(\vec{x}_2)$ let \vec{x}_1 be at unit radial distance from source, that is, at $R_1 = \cos\theta_1$ where θ_1 is the ray launch angle. Let $c(\vec{x}_1)$ be the reference sound speed, $A_0 = A(\vec{x}_1)$ the reference (source) amplitude. Then, $dz_1 \cos\theta_1 = d\theta$ implies that

$$A(\vec{x}_2) \approx \sqrt{\frac{1}{n(\vec{x}_2)} \frac{\cos\theta_1 d\theta}{R_2 \sin\theta_2 dR_2}} A_0.$$

One final cautionary note on the limits of the validity of ray theory must also be presented, and this is most easily developed within the context of a depth stratified medium ($c(\vec{x}) = c(z)$).

We notice that $A(\vec{x}) \sim \sqrt{c(\vec{x})} = \sqrt{c(z)}$; so, if we now also assume that we are away from turning points then $\nabla^2 A \approx A_{zz}$ and

$$\begin{aligned} A_{zz} &\approx \frac{d^2}{dz^2} \{c(z)\}^{1/2} \cdot A \Big|_{\text{turning point}} \\ &= \frac{1}{2} \left\{ \frac{d^2 c}{dz^2} c^{-1/2} - \frac{1}{2} c^{-3/2} \left(\frac{dc}{dz} \right)^2 \right\} \cdot A \Big|_{\text{turning point}}. \end{aligned} \tag{B8}$$

Thus $\frac{d^2 c}{dz^2}$ small leads to (with $A = \sqrt{c(z)} A|_{\text{turning point}}$)

$$\left| \frac{A_{zz}}{A} \right| \approx \frac{1}{4} c^{-2} \left(\frac{dc}{dz} \right)^2. \quad (\text{B9})$$

Therefore, $\left| \frac{\nabla^2 A}{A} \right| \frac{1}{4} c^{-2} \left(\frac{dc}{dz} \right)^2 \ll \frac{\omega^2}{c^2}$ leads to

$$\frac{1}{2\omega} \left| \frac{dc}{dz} \right| \ll 1. \quad (\text{B10})$$

This inequality (B10) illustrates an intuitive *low-gradient requirement* (necessary but not sufficient) for the ray approximation [B1,B2].

A wave-theoretical approach leading to an optical theoretic solution is to construct the Green's function in integral form, reexpress the function as a series in terms of traveling waves, and then reduce the integrals by means of saddle-point evaluations [B3,B4].

The present ray-theoretic model expands the parameters of interest for each ray, that is, range, depth, angle, travel time, Snell's "constant," by means of a Taylor series expansion (finite number of terms) expressed as a function of arc-length, l . These terms are evaluated by means of the ray equation:

$$\frac{d}{dl} \left(n \frac{d\vec{x}}{dS} \right) = \nabla n, \quad (\text{B11})$$

where l is the arc length along the ray, and by means of environmental data, that is, first- and second-order derivatives of $c(\vec{x})$ with respect to depth and range.

Equation (B11) can be derived rigorously from Fermat's principle (the ray is path of minimum travel time between two fixed points) by the calculus of variations. It can also be derived* from the eikonal equation by noting that the unit vector normal \hat{p} to the wavefront (surface of constant phase) is given by

$$\hat{p} = \frac{\vec{\nabla} S}{n} \quad (\text{B12})$$

(follows from $|\vec{\nabla} S|^2 = n^2$) and is also given by the unit ray tangent \hat{v} where

$$\hat{v} = \left(\frac{dx_1}{dl}, \frac{dx_2}{dl}, \frac{dx_3}{dl} \right), \quad (\text{B13})$$

where $(x_1(l), x_2(l), x_3(l))$ is point on the ray. Thus,

$$\frac{dx_i}{dl} = \frac{1}{n} \frac{\partial S}{\partial x_i}. \quad (\text{14})$$

*This derivation is courtesy of D. Berman (NRL).

Differentiating by l we get

$$\begin{aligned}
 \frac{d}{dl} \left(n \frac{dx_i}{dl} \right) &= \frac{d}{dl} \frac{\partial S}{\partial x_i} & (B15) \\
 &= \frac{\partial}{\partial x_i} \left(\frac{dS}{dl} \right) \\
 &= \frac{\partial}{\partial x_i} \left(\frac{\partial S}{\partial x_1} \frac{dx_1}{dl} + \frac{\partial S}{\partial x_2} \frac{dx_2}{dl} + \frac{\partial S}{\partial x_3} \frac{dx_3}{dl} \right) \\
 &= \frac{\partial}{\partial x_i} \left(\vec{\nabla} S \cdot \hat{v} \right) \\
 &= \frac{\partial}{\partial x_i} \left(\vec{\nabla} S \cdot \hat{p} \right) \\
 &= \frac{\partial}{\partial x_i} (n)
 \end{aligned}$$

since

$$\vec{\nabla} S = n\hat{p}.$$

The model used in this study assumes azimuthal symmetry for the environment and hence, it represents an approximate solution to the two-dimensional rather than to the full three-dimensional wave Eq. (A1) in Appendix A of this report.

In general ray theory has a number of advantages.

- It easily computes time of arrival for pulsed signals.
- It is versatile enough to handle complex geophysical conditions.
- Models for backscattering and forwardscattering of energy can be easily incorporated.
- It is an easily visualized technique.
- The equations are more tractable than, say, normal-mode equations, in a realistic environment.
- There is no limitation on the propagation angles which can be considered.

Of course ray theory also has its disadvantages.

- It does not predict well at low frequencies, for example,

$$\text{when } \lambda > \frac{h}{10},$$

where λ is signal wavelength, and

h is duct depth [B5],

or under strong gradient conditions when

$$\frac{1}{2\omega} \left| \frac{dc}{dz} \right| \geq 1,$$

where ω is angular source frequency,
 $c(r,z)$ is the sound speed profile,
 r is horizontal range,
 z is depth.

- The determination of appropriate rays (those connecting source and receiver) can be difficult or inefficient.
- The theory needs modification near caustics and focal points.
- Its predictions are very sensitive to discontinuities in the slopes and curvatures of the sound speed profiles [B6-B8].

The model used an automated ray-selection procedure which can be supplemented or replaced by user defined rays.

REFERENCES

- B1. I. Tolstoy and C.S. Clay, *Ocean Acoustics*, McGraw-Hill Book Co., 1966.
- B2. J.M. Pearson, *A Theory of Waves*, Allyn and Bacon, Inc., Boston, Mass., 1966.
- B3. L.B. Felsen and T. Ishihara, "Hybrid ray-mode formulation of ducted propagation," *JASA* **65**(3) 595-607 (1979).
- B4. L.B. Felsen and N. Marcuvitz, *Radiation and Scattering of Waves*, Prentice-Hall, 1973.
- B5. J.J. Cornyn, "GRASS: A Digital-Computer Ray-Tracing and Transmission-Loss-Prediction System, Volume I — Overall Description," NRL Report 7621, 1973.
- B6. M.A. Pedersen, "Acoustic Intensity Anomalies Introduced by Constant Velocity Gradients," *JASA* **33**(4) 465-474 (1961).
- B7. M.A. Pedersen and D.F. Gordon, "Comparison of Curvilinear and Linear Profile Approximation in the Calculation of Underwater Sound Intensities by Ray Theory," *JASA* **41**(2) 419-438 (1967).
- B8. H. Weinberg, "A Continuous-Gradient Curve-Fitting Technique for Acoustic-Ray Analysis," *JASA* **50**(3), 975-984 (1971).

Appendix C ANALYTIC PROFILE RESULTS

It can be shown [C1,C2] that a ray-theoretic solution should focus periodically and independently of launch angle when the sound-speed profile is of the form

$$c(z) = A \cosh B(z - C),$$

and when the source and receiver are located at the profile axis, that is, at $z = C$. For this test case we selected $A = 1500$ m/s, $B = 0.003$ m⁻¹, and $C = 1500$ m for a total water depth of 3000 m (Fig. C1). Figure C2a shows how well the ray model reproduces the predicted focusing. In contrast, Fig. C2b shows the lack of perfect focusing by the PE model for this profile. Next, we considered a profile for which the PE is predicted to focus perfectly, that is one for which the square of the index of refraction is parabolic. We matched this profile as closely as possible to the previous hyperbolic cosine profile,

$$c(z) = \frac{A}{\sqrt{-\beta(z - 1500)^2 + \alpha}},$$

where $c(0) = c(3000) = 1654.4 \rightarrow \alpha = 1$

$$\beta = 7.9 \times 10^{-8}$$

$$(\sqrt{\beta} \approx 2.8 \times 10^{-4}).$$

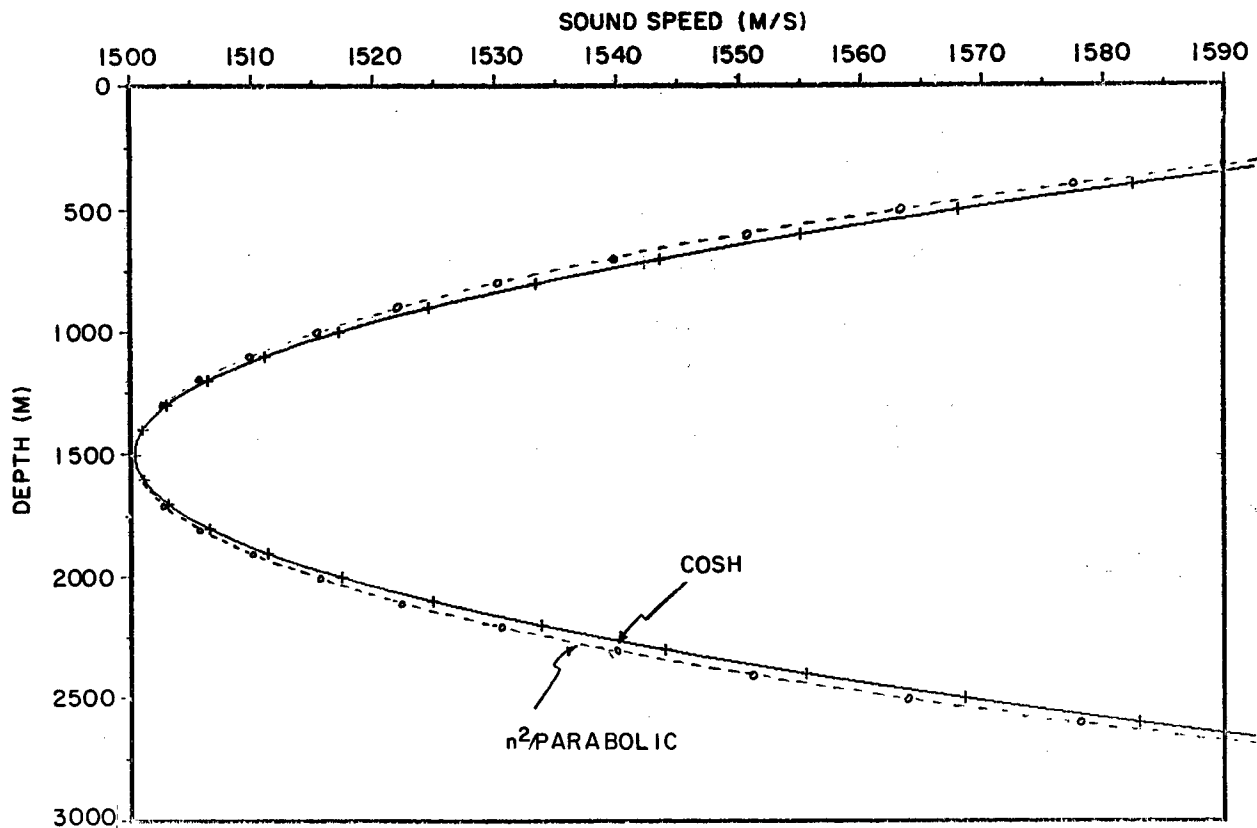


Fig. C.1 — Comparison of analytic profiles (hyperbolic cosine and n^2 parabolic)

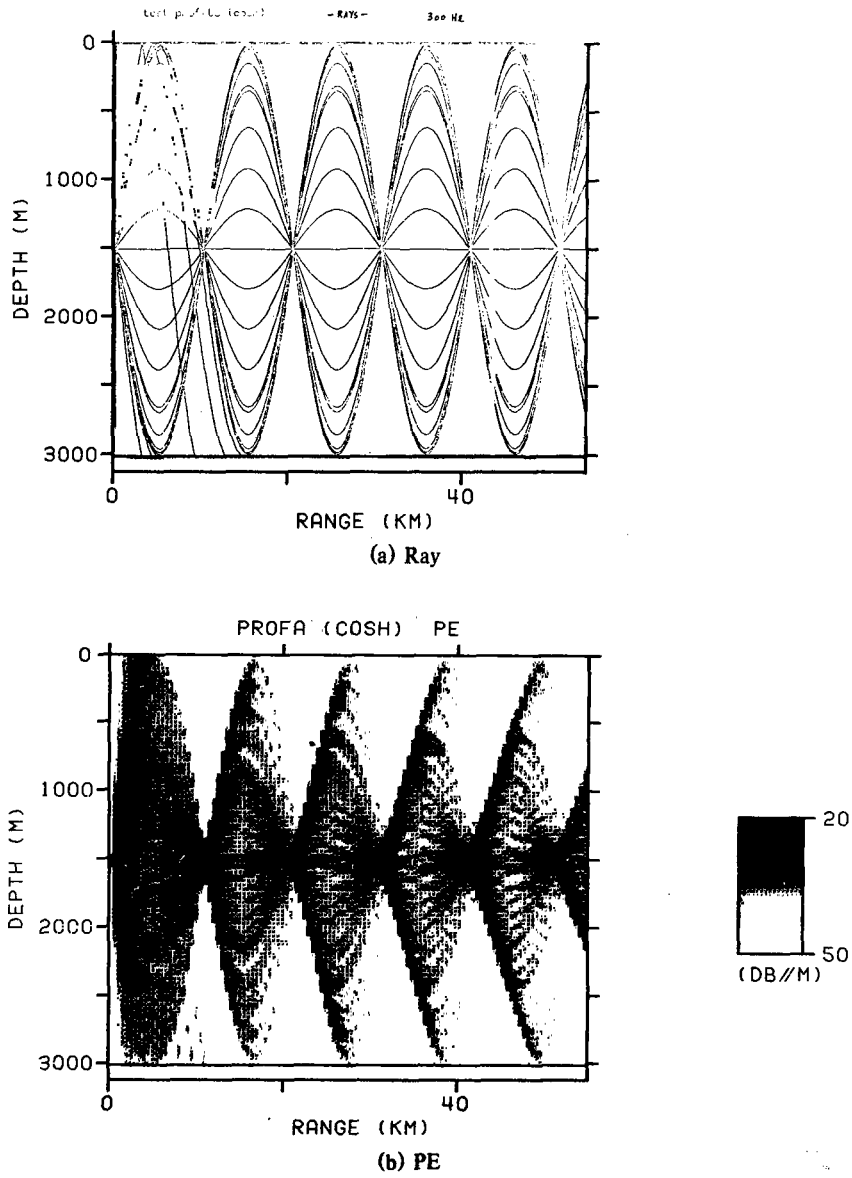


Fig. C.2 → Ray tracks and PE intensity plots for the hyperbolic cosine sound-speed profile with freq = 300 Hz

Note that if

$$\begin{aligned}
 f(x) &= \cosh bx \\
 &= \frac{e^{bx} + e^{-bx}}{2} \\
 &= \frac{1}{2} \left\{ \sum_{n=0}^{\infty} \frac{(bx)^n + (-bx)^n}{n!} \right\} \approx \frac{1}{2} [2 + (bx)^2] \\
 &= 1 + (1/2)(bx)^2.
 \end{aligned}$$

and

$$g(x) = \frac{1}{\sqrt{1 - \beta x^2}},$$

then .

$$f(x) \approx g(x) \text{ for } b^2 \approx \beta.$$

We have for the above examples $\sqrt{\beta} \approx 2.8 \times 10^{-4}$, $b = 3.0 \times 10^{-4}$ (Fig. C1). Then, in Fig. C3b we see the PE focusing perfectly while in Fig. C3a the ray model does not. This shift is also apparent in the TL vs range plots at a receiver depth of 100 m (Fig. C4a,b). Hence, we conclude that each model can react differently to the *same sound-speed environment* and show offsets between their respective interference patterns. Moreover, there is very little difference between these two analytical profiles, but that difference is sufficient to produce noticeable disagreements in the model predictions; yet the models are each performing exactly as they should. As a result, we should *not* expect perfectly correlated TL plots between the models for any given environments. Note that the analytic profiles selected here were much more refracting than one is likely to see in a real environment (min $c(z) = 1500.0$ m/s, max $c(z) = 1654.5$ m/s), and as such the model differences have been much more evident for these cases than one is likely to ever encounter in a realistic test.

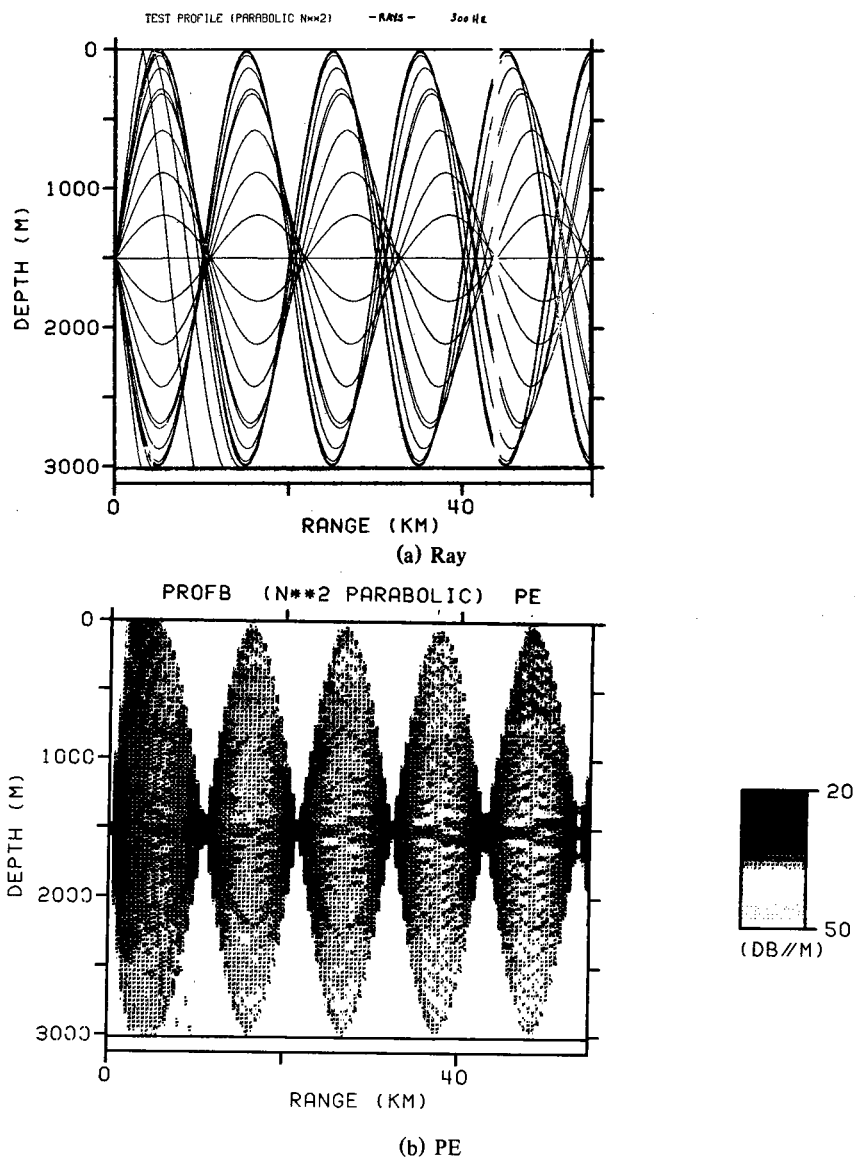


Fig. C.3 — Ray tracks and PE intensity plots for the n_2 parabolic sound-speed profile with freq = 300 Hz

TEST PROBE

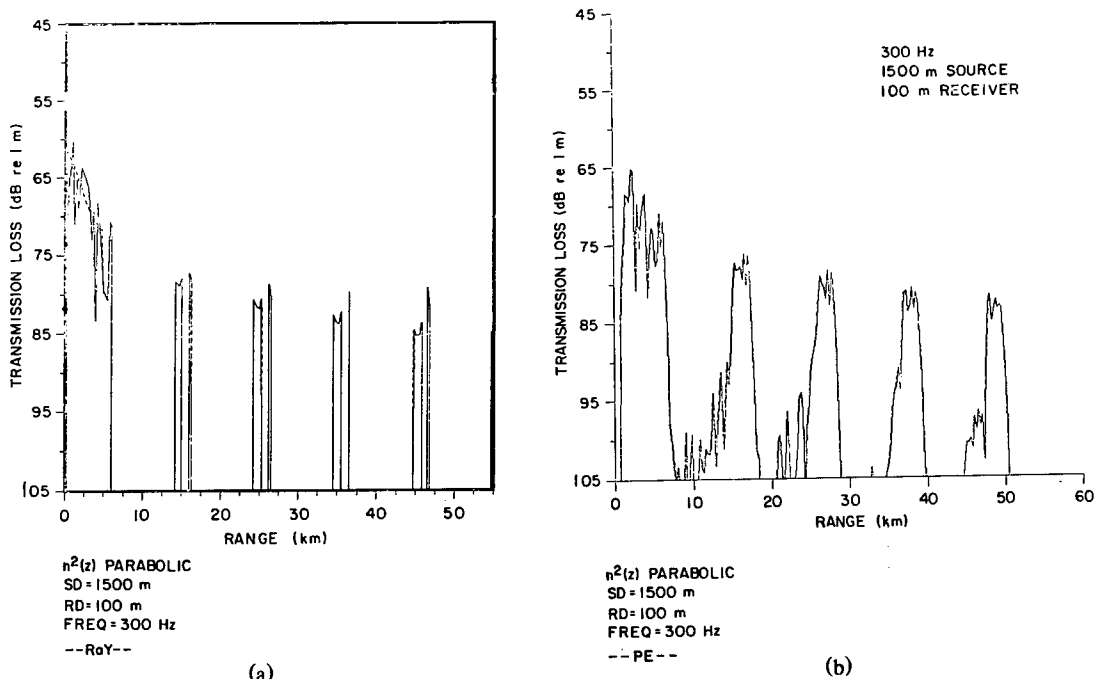


Fig. C.4 — Unaveraged transmission loss as a function of range (a: ray theoretic, b: PE theoretic) for the n^2 parabolic sound-speed profile with SD = 1500 m, RD = 100 m, freq = 300 Hz

REFERENCES

- C1. K.M. Guthrie, "The Propagation of Sofar Signals," Phd thesis, University of Auckland, New Zealand, 1974.
- C2. J.J. Cornyn, "GRASS: A Digital-Computer Ray-Tracing and Transmission-Loss-Prediction System," NRL Report 7621, 1973.